Acceleration of Amide Bond Rotation by Encapsulation in the Hydrophobic Interior of a Water-Soluble Supramolecular Assembly

Michael D. Pluth, Robert G. Bergman,[*] Kenneth N. Raymond[*]

Contribution from the Department of Chemistry, University of California, Berkeley, CA 94720-1460 and Chemistry Division, Lawrence Berkeley National Laboratory, Berkeley, California, 94720, USA

AUTHOR EMAIL ADDRESS: rgbergman@berkeley.edu, raymond@socrates.berkeley.edu

Prof. Robert G. Bergman, Prof. Kenneth N. Raymond, Department of Chemistry, University of California, Berkeley, CA 94720-1460 (USA). Fax: (+1) 510-642-7714 (Bergman). Fax: (+1) 510-486-5283 (Raymond). E-mail: rbergman@berkeley.edu, raymond@socrates.berkeley.edu

Abstract

The hydrophobic interior cavity of a self-assembled supramolecular assembly exploits the hydrophobic effect for the encapsulation of tertiary amides. Variable temperature ^{1}H NMR experiments reveal that the free energy barrier for rotation around the C-N amide bond is lowered by up to 3.6 kcal/mol upon encapsulation. The hydrophobic cavity of the assembly is able to stabilize the less polar transition state of the amide rotation process. Carbon-13 labeling studies showed that the ^{13}C NMR carbonyl resonance increases with temperature for the encapsulated amides which suggests that the assembly is able to favor a twisted for of the amide.

Introduction

The amide functional group plays an important role in the structure of proteins and is Nature's most fundamental connecting group.[1, 2] Although the exact nature of the electronic structure of the amide bond remains somewhat controversial,[3-8] addition of the carbonyl charge separation resonance structure to the classical resonance structures for the amide account for most of the characteristics of the amide bond (Figure 1a). Despite this controversy, many of the unique properties of amides, such as the hydrolytic stability and the high rotational barrier around the amide bond, stem from coplanarity of the atoms in the amide. Despite the large barrier to rotation around the amide C-N bond, Nature is able to catalyze the rotation using peptidylproline cis-trans isomerases (PPIases) such as cyclophilin and FK-506 binding protein.[9, 10] Structural studies have shown that the active site of FKBP contains hydrophobic side chains that are able to stabilize the hydrophobic transition state for amide bond rotation.[11-14] During amide bond rotation, the nitrogen and oxygen atoms must break conjugation which leads to a less polar transition state with respect to the ground state structure (Figure 1b). Accordingly, desolvation has been implicated as a significant contributor to the activity of PPIases and their ability to reduce the activation barrier for peptide bond rotation by up to 8 kcal/mol.[15]
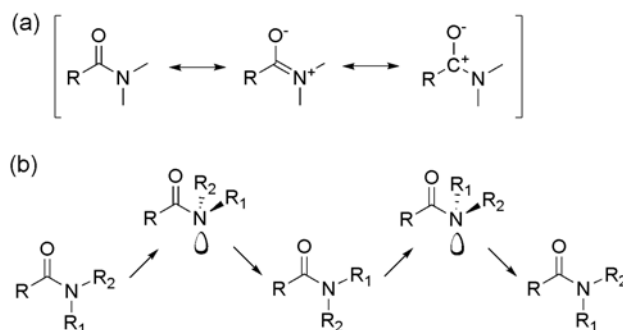

Figure 1 (a) Resonance structures for the amide bond. (b) Depiction of the rotational process of an amide bond which proceeds through an transition state with increased hydrophobic character.

Synthetic host molecules have proved useful in favoring reactivity which is effected by desolvation. For example, both natural cyclodextrins and a variety of synthetic supramolecular assemblies are able to encapsulate Diels-Alder reactants and increase the rate of the reaction. Similarly, the rotational behavior of amides has been investigated in synthetic host-guest systems by both the Cram and Rebek groups.[16, 17] In both cases, the amide rotational barrier was altered ($\leq$ 1.5 kcal/mol); either increasing or decreasing, depending on the substrate. This suggests that while the hydrophobicity of the transition state may be favored upon encapsulation, other forces are present which impede rotation and are of similar magnitude to the effects of hydrophobicity alone. Herein we report the use of a water-soluble supramolecular assembly to greatly reduce the barrier for amide bond rotation for encapsulated substrates

Results and Discussion

The tetrahedral supramolecular assembly $[Ga_4L_6]^{12-}$ (**1**, L = *N,N* -bis(2,3-dihydroxybenzoyl)-1,5-diaminonaphthalene) (Figure 2), has been investigated by the Raymond group over the last decade.[18-22] The 12⁻ overall charge of **1** imparts water solubility and the interior of **1** provides a hydrophobic cavity isolated from bulk solution. The tris-bidentate coordination at the metal vertices makes each vertex a stereocenter and the strong mechanical coupling of the ligands transfers the chirality of one metal vertex to the others forming the homochiral ΔΔΔΔ or ΛΛΛΛ isomers of the assembly. The hydrophobic interior has been exploited to encapsulate a variety of hydrophobic guests and has been used to stabilize species otherwise unstable in water, such as phosphine-acetone adducts, iminium cations, and tropylium.[23-25] We have previously exploited different aspects of the interior of **1** to affect chemical catalysis. The size constraints of the cavity have been used to pre-organize substrates into a reactive conformation for the [3,3] sigmatropic aza-Cope rearrangement[26, 27] and the preference for monocationic guests has facilitated the acid-catalyzed hydrolysis of orthoformates and acetals in basic solution.[28-30]
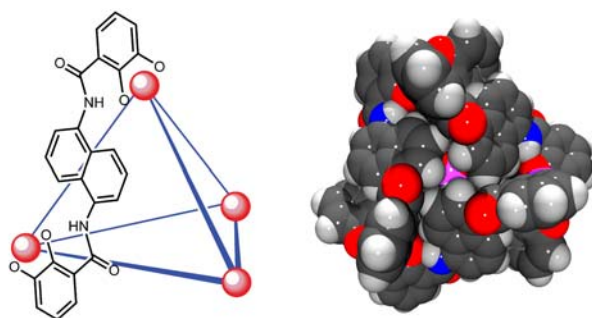

Figure 2. (Left) A schematic representation of **1** with only one ligand shown for clarity. (Right) A space-filling model of **1**.

Recent work from our laboratory has shown that the hydrophobic effect drives encapsulation of neutral guests in **1**.[31] This prompted our search for other transformations of neutral substrates which could be accelerated by **1**. With this in mind, we hoped that the hydrophobic cavity of **1** could stabilize the hydrophobic transition state for amide bond rotation. In order to test this hypothesis, *N,N*-diisopropylbenzamide (**2**) was encapsulated in **1** and its dynamic behavior probed with variable temperature ^{1}H NMR studies. Coalescence of the ^{1}H NMR resonances corresponding to encapsulated **2** was observed and the coalescence temperature was lower than for **2** in D_2O alone (Figure 3). Measurement of the coalescence temperature (T_c) and the difference in frequency of the coalescing peaks (Δv) enabled determination of the activation barrier for the bond rotation process.[32]
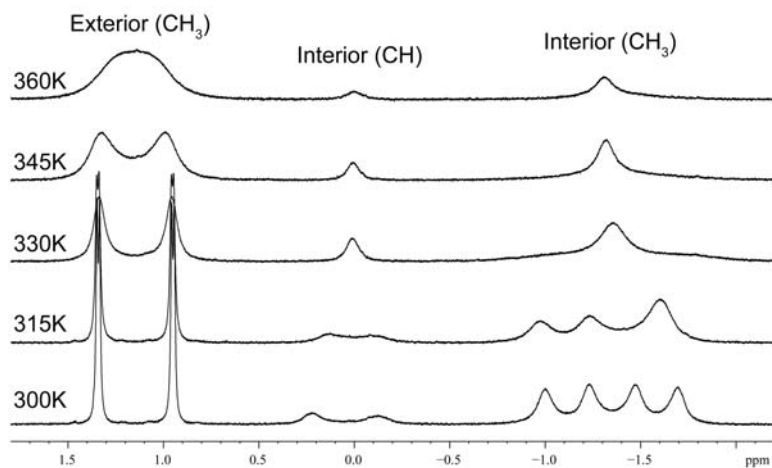
Figure 3 Variable temperature ^{1}H NMR spectra of $[2 \subset 1]^{12-}$.

The range of amides encapsulated in **1** was expanded by exposing suitable substrates to the assembly (Figure 4). Since the coalescence temperature was different for the amides in free solution and encapsulated in **1**, the assumption that $\Delta S^{\ddagger} \approx 0$ is necessary for comparison of the free energies, and is validated by the almost entirely enthalpic barrier for amide bond rotation.[33, 34] In all cases, a reduction in the barrier for amide bond rotation was observed upon encapsulation in **1** when compared to the free energy of rotation in D_2O solution. The difference upon encapsulation was greatest for *N,N*-dipropylnicotinamide (**8**), in which case the barrier for bond rotation was reduced by 3.6 kcal/mol (Table 1), corresponding to a rate acceleration of bond rotation by a factor of ~450.
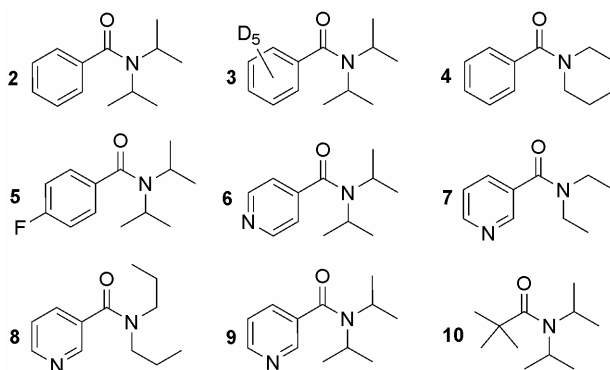

Figure 4 Scope of amides encapsulated in **1**.

Table 1 Activation barriers for amide bond rotation in D_2O, in **1**, and in toluene. (kcal/mol with uncertainty of $\pm$ 0.2 kcal/mol)

Guest	$\Delta G^{\ddagger}(D_2O)$	$\Delta G^{\ddagger}$ (in 1)	$\Delta G^{\ddagger}$ (Toluene)	$\Delta\Delta G^{\ddagger a}$
2	16.7	14.7	12.8	2.0
3	16.4	14.2	13.0	2.2
4	17.3	15.5	13.9	1.8
5	16.0	13.8	12.6	2.2
6	17.5	14.7	14.0	2.8
7	17.5	14.2	14.3	3.3
8	17.9	14.3	14.2	3.6
9	16.5	14.3	13.2	2.3
10	17.6	16.7	14.7	1.9

^{a} $\Delta\Delta G^{\ddagger} = \Delta G^{\ddagger}$ (D_2O) $- \Delta G^{\ddagger}$ (in **1**)

In order to investigate the maximum difference in rotation barrier based on hydrophobic effect alone, toluene was chosen as a solvent which should be similar to the interior of **1**. In all cases, the rotational barrier for amides in toluene was lower than in D_2O alone. Interestingly, the rotational barrier in toluene was less than or equal to that observed in **1** and provides a suitable experimental temperature range. If the acceleration of the bond rotation in **1** were solely due to the hydrophobic interior of **1**, then the rotational barrier would be expected to be identical for amides in toluene. However, this is not the case. The rotational barriers are generally lower in toluene which suggests that unfavorable steric interactions in **1** are likely present which attenuate the magnitude of the acceleration. Similarly, the alkyl groups on amides **7** and **8**, the amides with the greatest rotational barrier reduction in **1**, have the most flexibility and can attain conformations in **1** to avoid the unfavorable steric interactions. This suggests that although the interior of **1** hampers the rotational freedom of the encapsulated amide, it is the hydrophobicity of the cavity that dominates the reactivity.

In order to further probe the origin of the acceleration, carbon-13 labeling experiments were pursued. A number of reports in the literature have studied the relationship between the twist angle of amides and the $^{13}C\{^1H\}$ NMR shifts in solution.[35, 36] In general, the $^{13}C\{^1H\}$ chemical shift increases as a function of the amide twist angle. We verified these conclusions computationally for the model compound **2** using DFT NMR tensor calculations using Gaussian 03 (see supporting information).[37] For experimental measurements, ^{13}C-labeled **2** (^{13}C-**2**) was prepared by treating α-^{13}C-benzoylchloride with an excess of diisopropylamine.

Variable temperature ^{13}C NMR experiments in both D_2O and d_8-toluene revealed that the $^{13}C\{^1H\}$ chemical shift was unaffected by temperature. This suggests that although bond rotation was occurring, the ground state structure remained unchanged. However, a sizeable shift of over one ppm was observed for $[^{13}C$-**2** $\subset$ **1**$]^{12-}$ from 277K to 360K (Figure 5). During the experiment, the ^{13}C NMR shifts of the resonances corresponding to excess ^{13}C-**2** in solution did not change, thereby suggesting that guest exchange was not responsible for the ^{13}C shift. When compared to the theoretical studies on the effects of amide twist angle on the ^{13}C NMR shifts, these labeling studies suggest that encapsulation in **1** may perturb the potential energy surface for the bond rotation process and stabilize a more hydrophobic twisted form of the encapsulated amide.
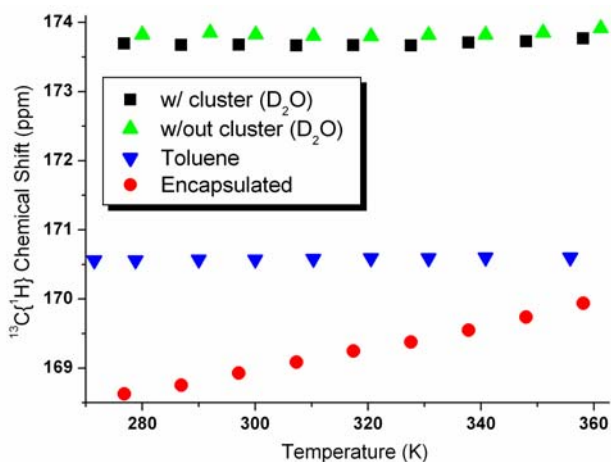
Figure 5 Observed $^{13}C\{^1H\}$ chemical shifts of **2** in D_2O both with and without, $[2 \subset 1]^{12-}$, in toluene, and encapsulated in **1**.

For example, if the potential energy surface for amide bond rotation by a dihedral angle of ϕ is approximated as a *sine* function with an activation barrier for rotation, *A*, (Figure 6), then the energy of any point on the potential energy surface for bond rotation is proportional to ϕ by the relationship shown in equation 1. Since amides are generally planar, the lowest energy structure has a twist angle of $\phi \sim 0$.
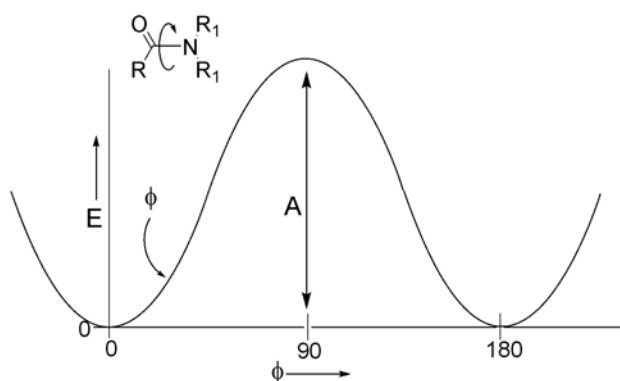

Figure 6. Approximation of the potential energy surface for amide bond rotation as a function of the twist angle ϕ.

$$E = A \, sin^2 \, \phi \tag{1}$$

Differentiating the expression in equation 1 with respect to ϕ allows for determination of the maxima and minima of the potential energy curve for amide bond rotation (equation 2). Further differentiation provides an expression for the force constant, *k*, corresponding to the dihedral rotational process around the C-N bond of the amide (equation 3).

6

$$\frac{\partial E}{\partial \phi} = 2A\, sin\, \phi\, cos\, \phi = A\, sin\, 2\phi \tag{2}$$

$$\frac{\partial^2 E}{\partial^2 \phi} = 2A\, cos\, 2\phi = k \tag{3}$$

Thus, in the planar form of an amide ($\phi \sim 0$) the energy surface for rotation around the C-N bond is symmetric and the force constant for dihedral rotation only depends on the activation barrier ($k = 2A$). However, if the lowest energy (E = 0) conformation of the amide is twisted rather than planar, ($\phi \neq 0$), the potential energy surface for dihedral rotation is more broad and is asymmetric ($k = 2Acos2\phi$) (Figure 7). The broader potential energy surface for dihedral rotation would account for, and is consistent with, the observed increase in $^{13}C\{^{1}H\}$ shift of the amide in **1**. Stabilization of a twisted form of encapsulated amides in **1** would result in destabilization of the ground state of the amide more than the transition state; this would consequently result in a lower rotational barrier for the amide encapsulation in **1**.
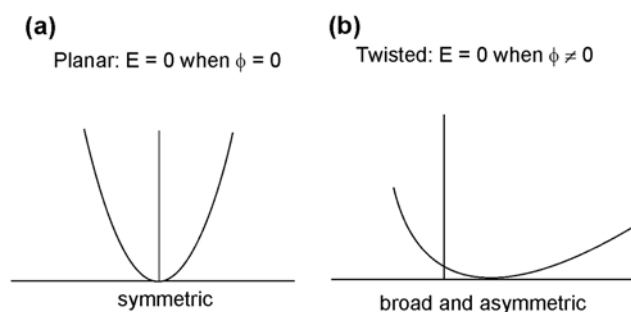

(a)
Planar: E = 0 when ϕ = 0

(b)
Twisted: E = 0 when $\phi \neq 0$

symmetric

broad and asymmetric

Figure 7 Comparison of the energy well for non twisted (a) and twisted (b) amides.

Conclusion

In summary, we have exploited the hydrophobic interior of a self-assembled supramolecular assembly to greatly accelerate the rotation of encapsulated amides. Variable temperature ^{13}C-NMR labeling experiments suggest that the potential energy surface of amide rotation inside of the assembly is considerably different from that in free solution and that ground state destabilization may contribute to the observed acceleration.

Experimental

General Procedures. All NMR spectra were obtained using a Bruker AV-500 MHz spectrometer at the indicated frequencies. Chemical shifts are reported as parts per million (δ) and referenced to residual acetone (for ^{1}H) and or a capillary of dioxane (^{13}C). Amides were prepared by addition of an excess of the corresponding secondary amine to the desired acid chloride. All amide products were purified by either distillation or recrystallization from hot hexanes. The following abbreviations are used in describing NMR couplings: (s) singlet, (d) doublet, (t) triplet, (q) quartet, b (broad), m (multiplet). The temperature of all variable temperature NMR experiments was calibrated with methanol or ethylene glycol standards.[38] Infrared (IR) spectra were recorded on a Nicolet 380 FT-IR spectrometer.

Determination of $\Delta G^{\ddagger}_{inv}$ using the coalescence temperature method. Analysis of coalescence data using lineshape analysis was not possible due to both encapsulation and guest exchange affecting the peak width of encapsulated substrates. Activation energies for rotation were determined using the coalescence method by determining the coalescence temperature (T_c) and chemical shift difference at the slow exchange limit ($\Delta \upsilon$) from equation (4). In all cases, when multiple decoalescing peaks could be followed, the activation barriers determined from the different peaks were identical. The uncertainty in $\Delta G^{\ddagger}_{inv}$ was calculated using differential error analysis by equation (5).

$$\Delta G^{\ddagger} = R \cdot T_c \cdot \ln\left(\frac{R \cdot T_c}{k_c \cdot N_A \cdot h}\right), \qquad k_c = \frac{\pi}{\sqrt{2}}\left|\Delta\upsilon\right| \tag{4}$$

$$\sigma(\Delta G^{\ddagger}_{inv}) = \sqrt{\left(\frac{\partial(\Delta G^{\ddagger}_{inv})}{\partial(\delta\upsilon)}\right)^2 \sigma^2(\Delta\upsilon) + \left(\frac{\partial(\Delta G^{\ddagger}_{inv})}{\partial(T_c)}\right)^2 \sigma^2(T_c)} \tag{5}$$

[^{13}C-N,N-diisopropylbenzamide] (^{13}C-2) To a 10 mL round bottom flask were added ^{13}C-benzoic acid (241 mg, 1.96 mmol), thionyl chloride (0.75 mL, 10.2 mmol) and DMF (15µl). The reaction mixture was allowed to stir for 30 minutes at which point it was heated to 50 C for 5 minutes then cooled to room temperature. The thionyl chloride was removed carefully under vacuum at which point 25 mL CH_2Cl_2 was added to the resultant oil. Diisopropylamine (2.2 mL, 16 mmol) was added with a syringe and the reaction mixture was stirred for an additional 30 minutes. The reaction mixture was then washed with 1N HCl (2 x 10 mL), 1N NaOH (2 x 10 mL) and brine (1 x 10 mL), dried over $MgSO_4$ and the solvent was removed under vacuum to yield a white powder. The crude product was dissolved in a minimal amount of boiling hexane (~3 mL) and filtered through a pre-heated glass wool plug. Slow cooling the filtrate to -70 ^{o}C yielded a white microcrystalline product which was dried under vacuum to give the title compound (285 mg, 71% yield). ^{1}H NMR (500 MHz, CDCl$_3$): 7.38 (m, 3H, 3 x CH), 7.32 (m, 2H, 2 x CH), 3.84 (bs, 1H, CH), 3.54 (bs, 1H, CH), 1.59 (bs, 6H, 2 x CH$_3$), 1.16 (bs, 6H, 2 x CH$_3$). ^{13}C{^{1}H} NMR (125 MHz, CDCl$_3$): 171.5 (^{13}C), 139.4 (d, J = 65 Hz), 129.0, 128,8 (d, J = 4.3 Hz), 126.0 (d, J = 1.4 Hz), 51.1 (bs, CH), 46.1 (bs, CH), 21.1 HRMS: obs (calc): 207.157870 (207.157844). IR [neat, ν_{max} (cm^{-1})]: 2992 (w), 2967 (m), 2931 (w), 1601 (w), 1584 (s, ν_{CO}), 1562 (w), 1471 (w), 1436 (s), 1361 (m), 1323 (s), 1211 (m), 1186 (w), 1156 (m), 1134 (m), 1095 (w), 1039 (w), 1026 (m), 780 (m), 733 (w), 706 (m). Mp. 70 – 71 ^{o}C.

[N,N-diisopropyl,d_5-benzamide] (3) To a 10 mL round bottom flask were added d_5-benzoic acid (323 mg, 2.54 mmol), thionyl chloride (2.0 mL, 27.4 mmol) and DMF (15µl). The reaction mixture was allowed to stir for 30 minutes at which point it was heated to 50 ^{o}C for 5 minutes then cooled to room temperature. The thionyl chloride was removed carefully under vacuum at which point 25 mL CH_2Cl_2 was added to the resultant oil. Diisopropylamine (3.5 mL, 25.0 mmol) was added with a syringe and the reaction mixture was stirred for an additional 30 minutes. The reaction mixture was then washed with 1N HCl (2 x 10 mL), 1N NaOH (2 x 10 mL) and brine (1 x 10 mL), dried over $MgSO_4$ and the solvent was removed under vacuum to yield a white powder. The crude product was dissolved in a minimal amount of boiling hexane and filtered through a pre-heated glass wool plug. Cooling the filtrate to -70 ^{o}C yielded a white microcrystalline product which was dried under vacuum to give the title compound (408 mg, 76% yield). ^{1}H NMR (500 MHz, (CD$_3$)$_2$CO): 3.70 (bs, 2H, 2 x CH), 1.32 (bs, 12H, 4 x CH$_3$). ^{2}H NMR (76.7 MHz, (CD$_3$)$_2$CO): 7.39 (bs, 3H, 3 x CH), 7.29 (bs, 2H, 2 x CH). ^{13}C{^{1}H} NMR (125 MHz, (CD$_3$)$_2$CO): 170.0, 139.4, 127.8 (t, J = 24.7 Hz), 127.7 (t, J = 24. 6 Hz), 125.0 (t, J = 24.6 Hz), 45.2, 19.9. HRMS: obs (calc): 211.185840 (211.185873). IR [neat, ν_{max} (cm^{-1})]: 2992 (w), 2967 (m), 2931 (w), 2872 (w), 1621 (s), 1567 (w), 1468 (w), 1449 (m), 1316 (s), 1222 (w), 1157 (w), 1135 (w), 1077 (w), 1033 (m), 847 (m), 813 (w), 777 (w), 748 (w), 677 (w) Mp. 69 – 70 ^{o}C.

General Procedure for Amide Encapsulation. In an N_2 glovebox, 15 mg of $K_{12}[Ga_4L_6]$ was added to an NMR tube at which point 0.5 mL of D_2O was added. An excess of the amide (10 mg or 10 μL) was added by syringe or as a solid and the NMR tube was shaken for 30 seconds. For host-guest complexes, the encapsulated guest resonances are generally shifted upfield by 2-3 ppm which is consistent with encapsulation. Depending on the chemical shift of aromatic guests, some of the guest resonances overlap with the assembly resonances.

[*N,N*-diisopropylbenzamide $\subset$ Ga$_4$L$_6$]$^{12-}$ ([2 $\subset$ 1]$^{12-}$) ^{1}H NMR (500 MHz, D$_2$O, 300K): 7.77 (d, *J* = 7.5 Hz, 12H, *aryl*), 7.65 (t, *J* = 8.0 Hz, 12H, *aryl*), 7.21 (d, *J* = 8.0 Hz, 12H, *aryl*), 6.69 (t, *J* = 8.0 Hz, 12H, *aryl*), 6.65 (d, *J* = 8.0 Hz, 12H, *aryl*), 6.49 (t, *J* = 7.6 Hz, 12H, *aryl*). Guest: 5.99 (t, *J* = 7.0 Hz, 1H, CH), 5.50 (t, *J* = 7.0 Hz, 2H, 2 x CH), 3.58 (bs, 2H, 2 x CH), 0.28 (s, 1H, CH), -0.06 (s, 1H, CH), -1.00 (s, 3H, CH$_3$), -1.23 (s, 3H, CH$_3$), -1.47 (s, 3H, CH$_3$), -1.80 (s, 3H, CH$_3$). ^{1}H NMR (500 MHz, D$_2$O, 330K): 7.83 (d, *J* = 7.5 Hz, 12H, *aryl*), 7.59 (t, *J* = 8.0 Hz, 12H, *aryl*), 7.22 (d, *J* = 8.0 Hz, 12H, *aryl*), 6.87 (t, *J* = 8.0 Hz, 12H, *aryl*), 6.65 (d, *J* = 7.6 Hz, 12H, *aryl*), 6.50 (t, *J* = 7.6 Hz, 12H, *aryl*). Guest: 5.82 (bs, 1H, CH), 5.65 (bs, 2H, 2 x CH), 3.35 (bs, 2H, 2 x CH), 0.01 (bs, 2H, 2 x CH), -1.35 (bs, 12H, 4 x CH$_3$).

[*N,N*-diisopropyl-*d$_5$*-benzamide $\subset$ Ga$_4$L$_6$]$^{12-}$ [3 $\subset$ 1]$^{12-}$ ^{1}H NMR (500 MHz, D$_2$O, 290K): 7.77 (d, *J* = 7.6 Hz, 12H, *aryl*), 7.72 (t, *J* = 8.0 Hz, 12H, *aryl*), 7.24 (d, *J* = 8.0 Hz, 12H, *aryl*), 6.93 (t, *J* = 8.0 Hz, 12H, *aryl*), 6.72 (d, *J* = 8.0 Hz, 12H, *aryl*), 6.55 (t, *J* = 7.6 Hz, 12H, *aryl*). Guest: 0.41 (s, 1H, CH), -0.17 (s, 1H, CH), -1.01 (s, 3H, CH$_3$), -1.17 (s, 3H, CH$_3$), -1.27 (s, 3H, CH$_3$), -1.75 (s, 3H, CH$_3$). ^{1}H NMR (500 MHz, D$_2$O, 325K): 7.87 (d, *J* = 7.5 Hz, 12H, *aryl*), 7.52 (t, *J* = 8.0 Hz, 12H, *aryl*), 7.25 (d, *J* = 8.0 Hz, 12H, *aryl*), 6.87 (t, *J* = 8.0 Hz, 12H, *aryl*), 6.63 (d, *J* = 7.4 Hz, 12H, *aryl*), 6.53 (t, *J* = 7.6 Hz, 12H, *aryl*). Guest: 0.04 (bs, 2H, 2 x CH), -1.38 (bs, 12H, 4 x CH$_3$).

[1-Benzoylpiperidine $\subset$ Ga$_4$L$_6$]$^{12-}$ ([4 $\subset$ 1]$^{12-}$) ^{1}H NMR (500 MHz, D$_2$O, 296K): 7.68 (bs, 24H, *aryl*), 7.16 (d, *J* = 7.6 Hz, 12H, *aryl*), 6.89 (bs, 12H, *aryl*), 6.65 (d, *J* = 7.4 Hz, 12H, *aryl*), 6.47 (t, *J* = 7.6 Hz, 12H, *aryl*). Guest: 5.98 (s, 1H, CH), 5.05 (s, 2H, 2 x CH), 4.30 (s, 2H, 2 x CH), -1.03 (s, 2H, CH$_2$), -1.14 (s, 2H, CH$_2$), -1.50 (s, 2H, CH$_2$), -1.92 (s, 2H, CH$_2$), -1.97 (s, 2H, CH$_2$). ^{1}H NMR (500 MHz, D$_2$O, 357K): 7.78 (bs, 12H, *aryl*), 7.62 (bs, 12H, *aryl*), 7.15 (bs, 12H, *aryl*), 6.90 (bs, 12H, *aryl*), 6.65 (bs, 12H, *aryl*), 6.46 (bs, 12H, *aryl*). Guest: 5,75 (s, 1H, CH), 5.19 (s, 2H, 2 x CH), 4.43 (s, 2H, 2 x CH), -0.90 (bs, 4H, 2 x CH$_2$), -1.52 (bs, 2H, CH$_2$), -1.85 (bs, 4H, 2 x CH$_2$).

[*N,N*-diisopropyl-*p*-fluorobenzamide $\subset$ Ga$_4$L$_6$]$^{12-}$ ([5 $\subset$ 1]$^{12-}$) ^{1}H NMR (500 MHz, D$_2$O, 277K): 7.17 (bs, 12H, *aryl*), 7.01 (bs, 12H, *aryl*), 6.78 (d, *J* = 7.5 Hz, 12H, *aryl*), 6.67 (d, *J* = 7.5 Hz, 12H, *aryl*), 6.57 (t, *J* = 8.0 Hz, 12H, *aryl*), 6.50 (bs, 12H, *aryl*). Guest: 5.05 (bs, 2H, 2 CH), 3.55 (s, 2H, 2 CH), 0.53 (bs, 1H, CH), -0.03 (bs, 1H, CH), -0.88 (bs, 3H, CH$_3$), -1.18 (bs, 3H, CH$_3$), -1.36 (bs, 3H, CH$_3$), -2.00 (bs, 3H, CH$_3$). ^{1}H NMR (500 MHz, D$_2$O, 332K): 7.87 (d, *J* = 7.5 Hz, 12H, *aryl*), 7.66 (d, *J* = 8.0 Hz, 12H, *aryl*), 7.18 (d, *J* = 8.0 Hz, 12H, *aryl*), 6.89 (t, *J* = 8.0 Hz, 12H, *aryl*), 6.62 (d, *J* = 8.0 Hz, 12H, *aryl*), 6.49 (t, *J* = 8.0 Hz, 12H, *aryl*). Guest: 5.36 (bs, 2H, 2 x CH), 3.79 (bs, 2H, 2 x CH), 0.04 (bs, 2H, 2 x CH), -1.30 (bs, 12H, 4 x CH$_3$).

[*N,N*-diisopropylisonicotinamide $\subset$ Ga$_4$L$_6$]$^{12-}$ ([6 $\subset$ 1]$^{12-}$) ^{1}H NMR (500 MHz, D$_2$O, 277K): 7.48 (d, *J* = 7.5 Hz, 12H, *aryl*), 7.35 (d, *J* = 8.0 Hz, 12H, *aryl*), 6.99 (d, *J* = 7.4 Hz, 12H, *aryl*), 6.38 (t, *J* = 8.0 Hz, 12H, *aryl*), 6.40 (d, *J* = 7.5 Hz, 12H, *aryl*), 6.22 (t, *J* = 7.5 Hz, 12H, *aryl*). Guest: 2 aryl H overlapping with host, 3.23 (s, 2H, 2 CH), 0.33 (s, 1H, CH), -0.09 (s, 1H, CH), -1.04 (s, 3H, CH$_3$), -1.18 (s, 3H, CH$_3$), -1.44 (s, 3H, CH$_3$), -1.99 (s, 3H, CH$_3$). ^{1}H NMR (500 MHz, D$_2$O, 340K): 7.76 (d, *J* = 8.0 Hz, 12H, *aryl*), 7.68 (d, *J* = 7.6 Hz, 12H, *aryl*), 7.17 (bs, 12H, *aryl*), 6.90 (d, *J* = 7.5 Hz, 12H, *aryl*), 6.60 (bs, 12H, *aryl*), 6.43 (t, *J* = 8.0 Hz, 12H, *aryl*). Guest: 2 aryl H overlapping with host, 3.84 (s, 2H, 2 x CH), -0.02 (bs, 2H, 2 x CH), -1.53 (bs, 12H, 4 x CH$_3$).

[*N,N*-diethylnicotinamide $\subset$ Ga$_4$L$_6$]$^{12-}$ ([7 $\subset$ 1]$^{12-}$) ^{1}H NMR (500 MHz, D$_2$O, 278K): 8.11 (bs, 12H, *aryl*), 7.28 (bs, 12H, *aryl*), 6.52 (bs, 12H, *aryl*), 6.35 (d, *J* = 7.4 Hz, 12H, *aryl*), 6.21 (bs, 12H, *aryl*), 6.14 (bs, 12H, *aryl*). Guest: 4.78 (s, 1H, CH), (other CH overlapping with cluster) -0.31 (s, 2H, CH$_2$), -

0.46 (s, 2H, CH$_2$), -1.57 (s, 3H, CH$_3$), -1.68 (s, 3H, CH$_3$). ^{1}H NMR (500 MHz, D$_2$O, 313K):   8.14 (d, J = 7.6 Hz, 12H, *aryl*), 7.21 (bs, 12H, *aryl*), 6.55 (t, J = 8.0 Hz, 12H, *aryl*), 6.31 (d, J = 7.4 Hz, 12H, *aryl*), 6.19 (t, J = 7.6 Hz, 12H, *aryl*), 6.12 (bs, 12H, *aryl*). Guest: 4.73 (s, 1H, CH), (other CH overlapping with cluster) -0.31(bs, 4H, 2 x CH$_2$), -1.62 (bs, 6H, 2 x CH$_3$).

[*N,N*-dipropylnicotinamide ⊂ Ga$_4$L$_6$]$^{12-}$ ([8 ⊂ 1]$^{12-}$) ^{1}H NMR (500 MHz, D$_2$O, 277K):   7.34 (bs, 12H, *aryl*), 7.13 (d, J = 8.0 Hz, 12H, *aryl*), 6.84 (bs, 12H, *aryl*), 6.61 (d, J = 8.0 Hz, 12H, *aryl*), 6.42 (bs, 12H, *aryl*), 6.18 (bs, 12H, *aryl*). Guest: 5.38 (s, 1H, CH), 5.22 (s, 1H, CH), 4.57 (s, 1H, CH), (other 2 CH overlapping with cluster), 0.08 (s, 2H, CH$_2$), -0.48 (s, 2H, CH$_2$), -0.81 (s, 2H, CH$_2$), -1.36 (s, 2H, CH$_2$), -1.41 (s, 3H, CH$_3$), -1.74 (s, 3H, CH$_3$). ^{1}H NMR (500 MHz, D$_2$O, 319K):   7.66 (d, J = 8.0 Hz, 12H, *aryl*), 7.37 (d, J = 8.0 Hz, 12H, *aryl*), 7.14 (bs, 12H, *aryl*), 6.86 (d, J = 8.0 Hz, 12H, *aryl*), 6.60 (bs, 12H, *aryl*), 6.42 (t, J = 7.6 Hz, 12H, *aryl*). Guest: 5.61 (s, 1H, CH), 5.58 (s, 1H, CH), 4.81 (s, 1H, CH), (other 2 CH overlapping with cluster), -0.10 (s, 4H, 2x CH$_2$), -0.90 (s, 4H, 2 x CH$_2$), -1.61 (s, 4H, 2 x CH$_2$).

[*N,N*-diisopropylnicotinamide ⊂ Ga$_4$L$_6$]$^{12-}$ ([9 ⊂ 1]$^{12-}$) ^{1}H NMR (500 MHz, D$_2$O, 277K):   7.78 (bs, 12H, *aryl*), 7.43 (bs, 12H, *aryl*), 7.17 (bs, 12H, *aryl*), 6.83 (bs, 12H, *aryl*), 6.73 (bs, 12H, *aryl*), 6.57 (bs, 12H, *aryl*). Guest: 5.07 (s, 1H, CH), 4.55 (s, 1H, CH), 3.20 − 3.26 (bs, 2H, 2 CH), 0.45 (s, 1H, CH), -0.01 (s, 1H, CH), -0.55 (s, 3H, CH$_3$), -0.81 (s, 3H, CH$_3$), -1.72 (s, 3H, CH$_3$), -1.95 (s, 3H, CH$_3$). ^{1}H NMR (500 MHz, D$_2$O, 322K):   7.89 (d, J = 7.5 Hz, 12H, *aryl*), 7.48 (d, J = 8.0 Hz, 12H, *aryl*), 7.31 (t, J = 7.5 Hz, 12H, *aryl*), 7.08 (t, J = 7.5 Hz, 12H, *aryl*), 6.73 (d, J = 7.5 Hz, 12H, *aryl*), 6.35 (t, J = 7.5 Hz, 12H, *aryl*). Guest: 5.15 (s, 1H, CH), 4.59 (s, 1H, CH), 3.47 (s, 1H, CH), 3.40 (s, 1H, CH), -0.23 (bs, 2H, 2 x CH), -1.27 (s, 12H, 4 x CH$_3$).

[*N,N*-diisopropylpivalamide ⊂ Ga$_4$L$_6$]$^{12-}$ ([10 ⊂ 1]$^{12-}$) ^{1}H NMR (500 MHz, D$_2$O, 277K):   7.98 (bs, 12H, *aryl*), 7.69 (bs, 12H, *aryl*), 7.29 (bs, 12H, *aryl*), 6.85 (bs, 12H, *aryl*), 6.65 (bs, 12H, *aryl*), 6.54 (bs, 12H, *aryl*). Guest: 0.50 (s, 1H, CH), -0.52 (s, 1H, CH), -1.36 (d, J = 7.0 Hz, 3H, CH$_3$), -1.46 (d, J = 7.0 Hz, 3H, CH$_3$), -1.59 (d, J = 7.0 Hz, 3H, CH$_3$), -1.62 (d, J = 7.0 Hz, 3H, CH$_3$), -1.75 (s, 9H, 3 x CH$_3$). ^{1}H NMR (500 MHz, D$_2$O, 346K):   7.94 (bs, 12H, *aryl*), 7.58 (d, J = 7.6 Hz, 12H, *aryl*), 7.26 (d, J = 8.0 Hz, 12H, *aryl*), 6.65 (bs, 12H, *aryl*), (other two cluster resonances overlapping with exterior guest), Guest: -0.04 (s, 2H, 2 x CH), -1.44 (bs, 12H, 4 x CH$_3$), -1.76 (s, 9H, 3 x CH$_3$).

Supporting Information Available: Computation details, NMR spectra, and complete Ref. 37. This material is available free of charge via the Internet at http://pubs.acs.org.

References

(1)   Fischer, G., *Angew. Chem. Int. Ed.* **1994,** *33*, 1415.
(2)   Lummis, S. C. R.; Beene, D. L.; Lee, L. W.; Lester, H. A.; Broadhurst, R. W.; Dougherty, D. A., *Nature* **2005,** *438*, 248.
(3)   Wiberg, K. B.; Breneman, C. L., *J. Am. Chem. Soc.* **1992,** *114*, 831.
(4)   Wiberg, K. B.; Laidig, K. E., *J. Am. Chem. Soc.* **1987,** *109*, 5935.
(5)   Perrin, C. L., *J. Am. Chem. Soc.* **1991,** *113*, 2865.
(6)   Gatti, C.; Fantucci, P., *J. Phys. Chem.* **1993,** *97*, 11677.
(7)   Laidig, K. E., *J. Am. Chem. Soc.* **1992,** *114*, 7912.
(8)   Lauvergnat, D.; Hiberty, P. C., *J. Am. Chem. Soc.* **1997,** *119*, 9478.
(9)   Fischer, G., *Chem. Soc. Rev.* **2000,** *29*, 119.

(10)   Mohanty, J.; Bhasikuttan, A. C.; Nau, W. M.; Pal, H., *J. Phys. Chem. B.* **2006,** *110*, 5132-5138.

(11)   Kallen, J.; Spitzfaden, C.; Zurini, M. G. M.; Wider, G.; Widmer, H.; Wuthrich, K.; Walkinshaw, M. D., *Nature* **1991,** *353*, 276.

(12)   Michnick, S. W.; Rosen, M. K.; Wandless, T. J.; Karplus, M.; Schreiber, S. L., *Science* **1991,** *252*, 836.

(13)   Moore, J. M.; Peattie, D. A.; Fitzgibbon, M. J.; Thompson, J. A., *Nature* **1991,** *351*, 248.

(14)   Van Duyne, G. D.; Standaert, R. F.; Karplus, P. A.; Schreiber, S. L.; Clardy, J., *Science* **1991,** *252*, 839.

(15)   Kofron, J. L.; Kuzmic, P.; Kishore, V.; Colon-Bonilla, E.; Rich, D. H., *Biochemistry* **1991,** *30*, 6127.

(16)   Salvio, R.; Moisan, L.; Ajami, D.; Rebek Jr., J., *Eur. J. Org. Chem.* **2007,** *16*, 2722.

(17)   Sherman, J. C.; Knobler, C. B.; Cram, D. J., *J. Am. Chem. Soc.* **1991,** *113*, 2194.

(18)   Caulder, D. L.; Powers, R. E.; Parac, T. N.; Raymond, K. N., *Angew. Chem. Int. Ed.* **1998,** *37*, 1840-1843.

(19)   Caulder, D. L.; Raymond, K. N., *Acc. Chem. Res.* **1999,** *32*, 975-982.

(20)   Davis, A. V.; Fiedler, D.; Seeber, G.; Zahl, A.; van Eldik, R.; Raymond, K. N., *J. Am. Chem. Soc.* **2006,** *128*, 1324-1333.

(21)   Davis, A. V.; Raymond, K. N., *J. Am. Chem. Soc.* **2005,** *127*, 7912-7919.

(22)   Fiedler, D.; Leung, D. H.; Bergman, R. G.; Raymond, K. N., *Acc. Chem. Res.* **2005,** *38*, 349.

(23)   Brumaghim, J. L.; Michels, M.; Pagliero, D.; Raymond, K. N., *Eur. J. Org. Chem.* **2004,** *24*, 5115.

(24)   Dong, V. M.; Fiedler, D.; Carl, B.; Bergman, R. G.; Raymond, K. N., *J. Am. Chem. Soc.* **2006,** *128*, 14464.

(25)   Ziegler, M.; Brumaghim, J. L.; Raymond, K. N., *Angew. Chem. Int. Ed.* **2000,** *39*, 4119.

(26)   Fiedler, D.; Bergman, R. G.; Raymond, K. N., *Angew. Chem. Int. Ed.* **2004,** *43*, 6748 - 6751.

(27)   Davis, A. V.; Fiedler, D.; Seeber, G.; Zahl, A.; van Eldik, R.; Raymond, K. N., *J. Am. Chem. Soc.* **2006,** *128*, 1324 - 1333.

(28)   Pluth, M. D.; Bergman, R. G.; Raymond, K. N., *Science* **2007,** *316*, 85-88.

(29)   Pluth, M. D.; Bergman, R. G.; Raymond, K. N., *J. Am. Chem. Soc.* **2007,** *129*, 11459-11467.

(30)   Pluth, M. D.; Bergman, R. G.; Raymond, K. N., *Angew. Chem. Int. Ed.* **2007,** *119*, 8741-8743.

(31)   Biros, S. M.; Bergman, R. G.; Raymond, K. N., *J. Am. Chem. Soc.* **2007,** *129*, 12094-12095.

(32)   Allerhand, A.; Gutowsky, H. S.; Jonas, J.; Meinzer, R. A., *J. Am. Chem. Soc.* **1966,** *88*, 3185.

(33)   Drakenberg, T.; Dahlqvist, K. I.; Forsen, S., *J. Phys. Chem.* **1972,** *76*, 2178.

(34)   Eberhardt, E. S.; Loh, S. N.; Hinck, A. P.; Raines, R. T., *J. Am. Chem. Soc.* **1992,** *114*, 5437.

(35)   Yamada, S., *Angew. Chem. Int. Ed.* **1995,** *24*, 1113.

(36)   Yamada, S., *J. Org. Chem.* **1996,** *61*, 941.

(37)   Frisch, M. J., et al. *Gaussian 03, Revision D.01*, Gaussian, Inc.: Wallingford CT, 2004.

(38)   Amman, C.; Meier, P.; Merbach, A. E., *J. Magn. Reson. A* **1982,** *46*, 319-321.